DFT Study of the Active Intermediate in the Fenton Reaction

Francesco Buda,*[a] Bernd Ensing,[a] Michiel C. M. Gribnau,[b] and Evert Jan Baerends*[a]

Abstract: Density functional theory has been used to investigate the nature of the oxidizing agent in the Fenton reaction. Starting from the primary intermediate $[Fe^{II}(H_2O)_5H_2O_2]^{2+}$, we show that the oxygen–oxygen bond breaking mechanism has a small activation energy and could therefore demonstrate the catalytic effect of the metal complex. The O–O bond cleavage of the coordinated H_2O_2, however, does not lead to a free hydroxyl radical. Instead, the leaving hydroxyl radical abstracts a hydrogen from an adjacent coordinated water leading to the formation of a second Fe–OH bond and of a water molecule. Along this reaction path the primary intermediate transforms into the $[Fe^{IV}(H_2O)_4(OH)_2]^{2+}$ complex and in a second step into a more stable high valent ferryl-oxo complex $[Fe^{IV}(H_2O)_5O]^{2+}$. We show that the energy profile along the reaction path is strongly affected by the presence of an extra water molecule located near the iron complex. The alternative intermediate $[Fe^{II}(H_2O)_4(OOH^-)(H_3O^+)]^{2+}$ suggested in the literature has been also investigated, but it is found to be unstable against the primary intermediate. Our results support a picture in which an Fe^{IV}-oxo complex is the most likely candidate as the active intermediate in the Fenton reaction, as indeed first proposed by Bray and Gorin already in 1932.

Keywords: catalysts · density functional calculations · Fenton reaction · oxidations

Introduction

It is more than a century since Fenton[1] first observed the powerful oxidizing properties of a mixture of Fe^{2+} ions and hydrogen peroxide in aqueous media. Surprisingly, the mechanism and the key intermediates in the Fenton chemistry remain, at present, open questions.[2, 3]

In the model proposed in the 1930s by Haber and Weiss,[4, 5] the oxidizing species is identified with free hydroxyl radicals ·OH produced by the iron-catalyzed decomposition of hydrogen peroxide:

$$Fe^{2+} + H_2O_2 \longrightarrow Fe^{3+} + OH^- + OH \quad (1)$$

This model, largely accepted for a long time, has been questioned by several experimental studies performed in the last two decades.[6–11] A direct detection of hydroxyl radicals by EPR is problematic because of their high reactivity resulting in a very short lifetime. Therefore these investigations rely generally on indirect approaches based on: i) trapping hydroxyl radicals to form a characteristic product[12] or ii) scavenging and kinetic experiments where reaction rates and reactivity patterns with a series of substrates are compared with those obtained in the presence of radiolytically generated hydroxyl radicals.[6] In the first approach, a spin trap, such as 5,5-dimethyl-1-pyrroline-*N*-oxide (DMPO), is used to form a stable ·OH radical adduct. The formation of a DMPO-OH adduct in a Fenton system[12] has been described as an evidence of the presence of free hydroxyl radical. However, it should be noted that a DMPO-OH adduct may be formed also by an iron–H_2O_2 complex reacting with DMPO.[13] The second approach relies on the presence of high precision data on the kinetics of the reaction and therefore requires a calibration by radiolysis studies for each case. Temperature and medium effects on the reaction rate often complicate the comparison. Furthermore, it is likely that the coordination environment of iron, and specifically the nature of the ligands, may strongly affect the stabilization of the reactive intermediate.[2] In many cases the results suggest the involvement of highly oxidizing iron intermediates which behave rather different from free ·OH. The primary step is assumed to consist of a nucleophilic addition of HOOH to the metal center to give the reactive intermediate of the Fenton reagents.[14] In most of the cases the exact nature of the reactive metal complex has not been clearly identified. Wink et al.[8] observed an intermediate in the oxidation of *N*-nitrosodimethylamine by the Fenton reagent in acidic aqueous solution which they identified with a peroxo species $Fe^{II}OOH$. Sawyer et al.[7, 9] have also suggested the formation

[a] Prof. E. J. Baerends, Dr. F. Buda, Ir. B. H. Ensing
Department of Theoretical Chemistry, Vrije Universiteit
De Boelelaan 1083, 1081 HV Amsterdam (The Netherlands)

[b] Dr. M. C. M. Gribnau
Unilever Research Vlaardingen
Postbus 114, Vlaardingen (The Netherlands)

  0947-6539/01/0713-2775 $ 17.50+.50/0

of a hydroperoxo complex by comparing relative reactivities of ·OH and Fenton oxidants with several hydrocarbon substrates in nonaqueous medium. A highly reactive intermediate $[Fe(OH)_2]^{2+}$ has been proposed by Rush and Koppenol,[6] which is assumed to be formed in the reaction between hydrogen peroxide and Fe^{II}HEDTA (hydroxyethylethylenediaminetriacetic acid) near neutral pH. More recently, Kremer[11] has suggested that a ferryl complex $[Fe^{IV}O]^{2+}$ acts as the key intermediate, by analysing the time dependence of the amount of O_2 evolved in the Fenton reaction. Indeed, a mechanism for the Fenton reaction based on a high-valent iron(IV)-oxo complex ($[Fe^{IV}O]^{2+}$) as the key intermediate was first suggested by Bray and Gorin[15] in 1932:

$$Fe^{2+} + H_2O_2 \longrightarrow FeO^{2+} + H_2O \qquad (2)$$

The issue on the prevalent mechanism in the Fenton reaction is also of great interest in the broader context of enzyme-catalyzed oxidation. It is in fact believed that metal-oxo or metal-peroxo species play a crucial role in both heme and non-heme based enzymes, such as cytochromes P450, non-heme oxygenases, the photosystem II, and also in DNA cleavage performed by activated bleomycin.[16]

A theoretical study can be helpful in discerning between different mechanisms and intermediates since it does not suffer from experimental limitations mainly due to the short life time of the active species. In this work we investigate the nature of the oxidizing intermediate in the Fenton reaction by using density functional theory (DFT)[17] calculations. We focus on the reaction in aqueous solution, that is, only water ligands are considered. We start from the assumption that a primary intermediate $[Fe^{II}(H_2O)_5H_2O_2]$ (**1**) is formed by exchange of a water molecule in the hydration shell of the hexa-aqua-Fe^{2+} complex by H_2O_2. We find that there is a specific reaction pathway along which the oxygen–oxygen bond breaking in this complex has an activation energy which is ten times smaller than for H_2O_2 in the vacuum. An interpretation of this catalytic effect of the metal center is given in terms of the bonding energies between the Fe ion and different ligand species. The oxygen–oxygen bond breaking is concomitant with the formation of a water molecule and the initial complex decays into a secondary intermediate **2**:

$$[(H_2O)_5Fe^{II}(H_2O_2)]^{2+}\ (\mathbf{1}) \longrightarrow [(H_2O)_4Fe^{IV}(OH)_2]^{2+}\ (\mathbf{2}) + H_2O \qquad (3)$$

This secondary intermediate **2** may further transform into an iron-oxo complex **3** with an activation barrier which is very small in the presence of an additional (non coordinated) water molecule:

$$[(H_2O)_4Fe^{IV}(OH)_2]^{2+}\ (\mathbf{2}) + H_2O \longrightarrow [(H_2O)_5Fe^{IV}O]^{2+}\ (\mathbf{3}) + H_2O \qquad (4)$$

The possible role of the solvent in this process has been investigated by introducing one or a few water molecules in the second coordination shell. The alternative intermediate $[Fe^{II}(H_2O)_4(OOH^-)(H_3O^+)]^{2+}$ suggested in the literature[7, 9] has been found to be unstable against the primary intermediate. The reaction path observed from **1** to **3** supports a picture of the Fenton reaction in which free hydroxyl radicals do not play a crucial role, and suggests a high-valent Fe^{IV} oxo complex as the most stable intermediate. Preliminary calculations actually show that this complex is very reactive in the presence of an organic substrate. These results will be the subject of a forthcoming paper.

Methods and Calculations

The Density functional theory calculations are performed using the ADF (Amsterdam density functional) code.[18] We use the generalized gradient approximation (GGA) in the form proposed by Perdew and Wang in 1991.[19] We have repeated some calculations with a different GGA (Becke–erdew)[20, 21] to test the dependence on the particular functional used: The results are unchanged by such choice. In the ADF code the electronic orbitals are written in terms of Slater-type orbitals (STO). We use a triple-zeta basis set with one polarization function (this choice corresponds to the basis set IV in the ADF package). The orbital 1s of oxygen and the orbitals up to the 3p of Fe are included as core functions in the calculations.

$[Fe^{II}(H_2O)_6]^{2+}$: We performed preliminary calculations on the hexa-aqua Fe^{II} complex and compared the results with available experimental data[22] to check the accuracy of the GGA functional for this system. We have optimized the geometry of this complex for different spin states. In agreement with experiment,[22] we find that the high-spin electronic state, with four unpaired spins ($S = 2$), is the ground state. The zero spin state ($S = 0$) is 26 kcal mol^{-1} higher in energy than the $S = 2$. In the minimum energy configuration the ferrous complex has a D_{2h} symmetry[23] with the six water ligands pseudo-octahedrally surrounding Fe. Figure 1 shows how the water ligands are oriented in order to minimize the mutual steric interaction.

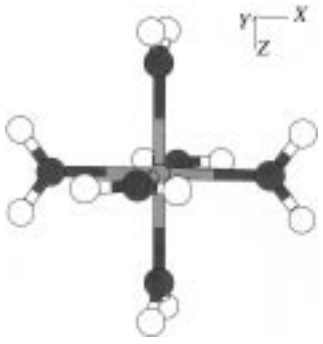

Figure 1. The D_{2h} geometry of the $[Fe(H_2O)_6]^{2+}$ complex. The relative orientation of the water ligands which minimizes the mutual steric interaction.

In the $S = 0$ electronic state the t_{2g} (d_{xy}, d_{xz}, d_{yz}) orbitals are fully occupied, while the e_g (d_{z^2}, $d_{x^2-y^2}$) orbitals are empty. The orbital energy difference between the t_{2g} and the e_g orbitals is 1.40 eV (cf. the ligand-field splitting in the octahedral symmetry). The six Fe–O bondlengths are all equal to 2.03 Å for this $(t_{2g})^6 (e_g)^0$ configuration. A molecular orbital

0947-6539/01/0713-2776 $ 17.50+.50/0 *Chem. Eur. J.* **2001**, *7*, No. 13

analysis shows that the $3d-t_{2g}$ states have π overlap with the highest occupied molecular orbital (HOMO) of the water ligands which corresponds to the π_{lp} lone pair of H_2O orthogonal to the plane of the molecule. This is an occupied–occupied orbital interaction, and therefore repulsive. The e_g states in the other hand have an overlap with the HOMO $-$ 1 orbital of the water ligands which corresponds to the σ_{lp} lone pair of H_2O located in the plane of the molecule. This σ-donation interaction is attractive. A Mulliken population analysis gives a net positive charge on the iron equal to $Q(Fe) = 0.68$, which corresponds to an electronic charge donation from the σ_{lp} orbital of 0.22 electrons per water molecule. The energy necessary to rotate one water ligand by 90° around the Fe–O axis amounts to 5 kcal mol^{-1} while keeping all the other degrees of freedom fixed. This effect can be attributed to steric repulsion by the neighboring H_2O ligands.

In the high-spin configuration $(t_{2g})^4(e_g)^2$ ($S = 2$) only one of the three t_{2g} orbitals is doubly occupied. Therefore we have three energetically degenerate configurations: $(d_{xy})^2\ d_{xz}{}^{\uparrow} d_{yz}{}^{\uparrow}\ d_z{}^{2\uparrow}\ d_{x^2-y^2}{}^{\uparrow}$, $(d_{xz})^2\ d_{xy}{}^{\uparrow}\ d_{yz}{}^{\uparrow}\ d_z{}^{2\uparrow}\ d_{x^2-y^2}{}^{\uparrow}$, and $(d_{yz})^2\ d_{xy}{}^{\uparrow}\ d_{xz}{}^{\uparrow}\ d_z{}^{2\uparrow}\ d_{x^2-y^2}{}^{\uparrow}$. In each case the optimized geometry of the complex has two Fe–O bonds elongated with respect to the other four. Specifically, the Fe–O bond lengths are 2.14 Å (×4) and 2.23 Å (×2). The elongation occurs along the axis where the π_{lp} orbitals of the coordinated H_2O molecules have antibonding interaction with the doubly occupied t_{2g} orbital, that is, in the conformation of Figure 1, along the x direction, if d_{xy} is doubly occupied, along z if d_{xz} is doubly occupied, along y if d_{yz} is doubly occupied. At finite temperature a dynamical Jahn–Teller distortion might occur and the experimentally measured Fe–O bond length would then correspond to an average value. The average Fe–O bond length is in reasonable agreement with the experimental value of 2.12 Å[22] taking into account that our results are obtained for the complex in the vacuum, thus ignoring the effects of the environment (e.g. the counterion present in the crystalline phase). The larger Fe–O bond lengths in the $S = 2$ configuration lead to a lower energy cost to rotate one water ligand by 90°, that is 2 kcal mol^{-1} for the water ligands along the elongated axis, and 3 kcal mol^{-1} for a water ligand along the short axis. The larger distances will also lead to smaller overlap between the σ_{lp} orbitals of the water ligands and the e_g-type d acceptor orbitals. Indeed, Mulliken population gives a net positive charge on the iron of $Q(Fe) = 0.88$; this indicates a lower σ_{lp} charge donation than in the $S = 0$ state.

The one-electron energies and the composition of the highest occupied and lowest unoccupied molecular orbitals for $S = 2$ are shown in Table 1. Note that the majority of up-spin electrons leads to a strongly stabilizing exchange potential for the up-spin orbitals, all the up-spin d orbitals being below the down-spin ones. The double occupancy of d_{xz} destabilizes the up-spin orbital, so that this t_{2g}-type orbital ends up in between the e_g-type $d_{x^2-y^2}$ and $d_z{}^2$. The set of down-spin d orbitals is unoccupied except for the d_{xz}, which is actually the highest occupied orbital. The down-spin orbitals have the typical t_{2g} below e_g ordering.

We have also evaluated the first bond dissociation energy (FBDE) in the ferrous hexa-aqua complex. We find a value of 35.9 kcal mol^{-1} for $S = 0$ and the lower value of 24.5 kcal mol^{-1} for $S = 2$ in accordance with the occupation of the more strongly antibonding e_g orbitals. The five-coordinate complex stays in the octahedral geometry with an open site in the $S = 0$ state, while in the $S = 2$ state a trigonal-bipyramid structure is very slightly preferred, by 1 kcal mol^{-1}. In spite of the FBDE of 24.5, it is easy to create an open coordination site because a five-coordinate complex with one additional water molecule located in the second coordination shell is found to be almost isoenergetic to the six-coordinate complex in the high spin state.[24] Figure 2 shows the optimized geometry of this complex. The main reason why the complex in Figure 2 is almost isoenergetic to the hexa-aqua complex is that the additional water in the second shell forms a strong bond with one water ligand, with an O···O distance of 2.54 Å. This distance is much shorter than the 2.88 Å found for the typical hydrogen bond in a water dimer using the same functional. The bond strength—compensating for the FBDE of 24.5 kcal mol^{-1}—is also much larger than the typical hydrogen bond strength of 4 kcal mol^{-1}. An analysis of the different energy contributions shows that the electrostatic contribution to the H_2O–$[Fe(H_2O)_5]^{2+}$ bond is much higher in comparison to that found in a water dimer. This finding is important since it indicates that in the hexa-aqua complex it is easy to create an open coordination site, thus allowing for a ligand exchange.

Table 1. One-electron energies and percent composition of the lowest unoccupied and highest occupied molecular orbitals of $[Fe^{II}(H_2O)_6]^{2+}$ in the $S = 2$ state with d_{xz} doubly occupied in terms of Fe and water fragments.

Orbital	ε [eV]	Fe	H_2O
		occupied orbitals	
$3b_3 \cdot g\uparrow$	−15.87	54 d_{yz}	45 π (HOMO) waters along y
$3b_1 \cdot g\uparrow$	−15.81	50 d_{xy}	49 π (HOMO) waters along x
$7a_1 \cdot g\uparrow$	−15.16	45 $d_{x^2-y^2}$, 27 d_{z^2}	22 σ (HOMO − 1)
$3b_2 \cdot g\uparrow$	−14.59	85 d_{xz}	14 π (HOMO) waters along z
$8a_1 \cdot g\uparrow$	−14.48	49 d_{z^2}, 28 $d_{x^2-y^2}$	20 σ (HOMO − 1)
$3b_2 \cdot g\downarrow$	−12.69	95 d_{xz}	4 π (HOMO) waters along z
		unoccupied orbitals	
$3b_1 \cdot g\downarrow$	−12.27	95 d_{xy}	4 π (HOMO) waters along x
$3b_3 \cdot g\downarrow$	−12.26	95 d_{yz}	4 π (HOMO) waters along y
$7a_1 \cdot g\downarrow$	−11.61	59 $d_{x^2-y^2}$, 29 d_{z^2}	5 σ (HOMO − 1)
$8a_1 \cdot g\downarrow$	−10.51	28 $d_{x^2-y^2}$, 61 d_{z^2}	5 σ (HOMO − 1)
$9a_1 \cdot g\uparrow$	−9.34	25 4s	75 $3a_1$ (LUMO)
$9a_1 \cdot g\downarrow$	−9.18	18 4s	82 $3a_1$ (LUMO)

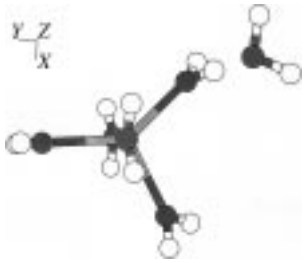

Figure 2. The optimized geometry of the $[Fe(H_2O)_5]^{2+}$ complex in the $S = 2$ state with an extra water molecule in the second coordination shell.

H_2O_2 in the vacuum: Since we are interested in the dissociation of hydrogen peroxide catalyzed by ferrous ion, we have computed first the geometry of H_2O_2 (see Table 2)

Table 2. Computed geometric parameters of the $[Fe^{II}(H_2O)_5H_2O_2]^{2+}$ complex in the low- and high-spin states. For comparison we show also the computed and the experimental[27] geometry of H_2O_2 in the vacuum. Distances are in Å, angles in degrees. δ (H-O-O-H) indicates the dihedral angle. The atomic numbering is the same as in Figure 3.

	$Fe^{II}(H_2O)_5H_2O_2$		H_2O_2	
	$S=0$	$S=2$	ADF	exptl
$Fe-O_{water}$	2.03 × 4, 2.00 (Fe – O2)	2.14 × 3, 2.12 (O2), 2.23 (O5)		
Fe–O6	1.94	2.21		
O6–O7	1.542	1.483	1.477	1.475
O6–H18, O7–H19	0.984	0.984, 0.986	0.978	0.950
∢ (H-O-O)	100.1, 96.9	100.1, 100.7	99.4	94.8
δ (H-O-O-H)	108.5	99.7	109.8	116.0
O7–H10	1.91	2.06		
O4–H18	2.45	3.00		
∢ (Fe-O6-O7)	115.0	113.3		

and the HO–OH bond dissociation energy in the vacuum. In particular, as is well known, we find that the H_2O_2 molecule is nonplanar with a twist angle of about 110° (point symmetry C_2). The nonplanarity of this molecule can be qualitatively understood by a molecular orbital analysis.[25] Since we are interested in the O–O bond cleavage, we take a slightly different route, using two ·OH radicals as building blocks (see Scheme 1 and Table 3). The ·OH radical has an unpaired

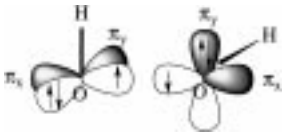

Scheme 1. ·OH Radicals as building blocks.

Table 3. One-electron energies and percent composition of the lowest unoccupied and occupied molecular orbitals of H_2O_2 in terms of ·OH radical fragments. The point symmetry is C_2. We assume that in the fragment the O–H bond is oriented along the z axis and that the SOMO is the π_x orbital (see also Scheme 1).

Orbital	ε [eV]	·OH
	occupied orbitals	
1a	– 27.99	91 1σ, 8 π_x (bonding)
1b	– 22.60	99 1σ (antibonding)
2a	– 13.39	54 2σ, 34 π_x (bonding)
2b	– 12.03	81 2σ, 11 π_y 6 π_x (antibonding)
3a	– 10.39	48 π_x, 25 2σ, 23 π_y (bonding)
4a	– 7.54	73 π_y, 19 2σ, 8 π_x (bonding)
3b	– 6.65	89 π_y, 11 2σ (antibonding)
	unoccupied orbitals	
4b	– 1.79	85 π_x, 8 3σ (antibonding)
5a	– 0.62	100 3σ, (bonding)
5b	0.69	100 3σ (antibonding)

electron in one of the π orbitals (π_x), and the O–O bond is basically an electron pair bond between these singly occupied orbitals. In order to avoid Pauli repulsion between the π_y lone pairs and between the O–H bond orbitals, rotation around the O–O bond axis over 90° (cf. Scheme 1) brings these orbitals to zero or small overlap. Since there is also repulsion between a π_y lone pair and an O–H bond orbital, the dihedral H-O-O-H angle does not become exactly 90°, each O–H bond rotates a further 9°. Repulsion is also decreased by the O–H axes rotating 10° outwards, increasing the O-O-H angle to 100°. The shape of hydrogen peroxide can thus be understood straightforwardly from the σ bond (p_σ+p_σ) formed by the π_x orbitals along the O–O axis, slightly strained by the increase of the O-O-H angle to 100°. The HOMO – 1 and HOMO of H_2O_2 correspond to the bonding and antibonding combinations of the doubly occupied π_y orbitals of the ·OH radicals, respectively, though a small mixing with other orbitals is present. The splitting between these two orbitals is small due to the small overlap between the π_y orbitals (see Scheme 1). The bonding and antibonding combinations of the strongly overlapping π_x orbitals exhibit a much larger splitting. The antibonding combination is the lowest unoccupied molecular orbital (LUMO). The bonding combination, constituting the σ bond formed between the two π_x singly occupied orbitals of the ·OH radicals, enters mostly the 3a (HOMO – 2) and 2a orbitals, see Table 3. Its bonding character lowers it sufficiently to come close to, and mix with, the O–H bonding orbital 2σ. This mixing leads to lowering of the 2a (mostly 2σ) and raising of the 3a (mostly π_x). Notably the LUMO of H_2O_2, occupation of which will weaken the O ··· O bond, is 1 eV lower in energy than the LUMO of H_2O.

The computed energy needed to break the O–O bond in the isolated H_2O_2 molecule is 61.8 kcal mol^{-1}. The inclusion of the zero-point energy correction gives 56.0 kcal mol^{-1}, in reasonable agreement with the experimental value at 25 °C of 51 kcal mol^{-1}.[26]

Results

Primary intermediate $[Fe^{II}(H_2O)_5H_2O_2]^{2+}$: We assume, as is usually done, that the first chemical step in the Fenton reaction is the nucleophilic addition of H_2O_2 to the iron complex by exchanging with a water ligand in the hydration shell.[14] Therefore we characterize the structural and electronic properties of the $[Fe^{II}(H_2O)_5H_2O_2]^{2+}$ complex (**1**). We find that the high spin configuration ($S=2$) is the most stable for the complex **1**, as it was the case for the hexa-aqua complex. Specifically, the $S=2$ state is 21.3 kcal mol^{-1} lower than the $S=0$ state. The calculated FBDE for a water ligand in **1** is 25 kcal mol^{-1}, which is the same value found for the hexa-aqua complex. The FBDE for the H_2O_2 ligand is about 27 kcal mol^{-1}, thus showing that the assumed exchange of a H_2O with a H_2O_2 ligand in the first hydration shell of iron(II) is thermodynamically slightly favored.

The optimized geometry in the $S=2$ spin configuration is shown in Figure 3, where the atomic numbering used in this work is also indicated. The relevant geometric parameters are summarized in Table 2. In Table 4 and Table 5 we show the molecular orbital analysis for the complex **1** in the $S=0$ and $S=2$ states, respectively. The H_2O_2 ligand stands in the "end-on" configuration. Indeed, we find that the complex with the H_2O_2 ligand in a "side-on" configuration (with the two O atoms at the same distance from the Fe) has an energy about 20 kcal mol^{-1} higher than the "end-on" and is a saddle point in

0947-6539/01/0713-2778 $ 17.50+.50/0 *Chem. Eur. J.* **2001**, *7*, No. 13

Table 4. One-electron energies and percent composition of the lowest unoccupied and highest occupied molecular orbitals of $[Fe^{II}(H_2O)_5H_2O_2]^{2+}$ in the $S=0$ state in terms of Fe, water and hydrogen peroxide fragments.

Orbital	ε [eV]	Fe	H_2O	H_2O_2
	occupied orbitals			
27a	−15.84			62 HOMO, 31 HOMO − 1
28a	−13.76	84 d_{xz}	4 π (HOMO) waters along z	6 LUMO
29a	−13.49	89 d_{xy}	8 π (HOMO) waters along x	
30a	−13.34	87 d_{yz}	6 π (HOMO) waters along y	
	unoccupied orbitals			
31a	−11.97	76 $d_{x^2-y^2}$, 6 d_{z^2}	14 σ (HOMO − 1) waters in the (xy) plane	
32a	−11.83	51 d_{z^2}, 7 $d_{x^2-y^2}$	8 σ (HOMO − 1) waters in the (yz) plane	23 LUMO, 5 HOMO
33a	−11.41	22 d_{z^2}, 4 d_{xz}		65 LUMO
34a	−9.34		79 LUMO	

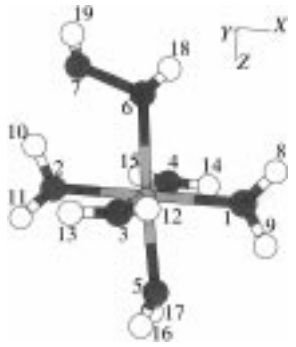

Figure 3. Optimized geometry of the primary intermediate (**1**) $[Fe^{II}(H_2O)_5H_2O_2]^{2+}$ in the high-spin ($S=2$) state showing the numbering system used in this paper and the orientation of the axes. The dark (white) balls are the oxygen (hydrogen) atoms.

the energy surface. The D_{2h} symmetry of the hexa-aqua complex is broken in the complex **1** by the H_2O_2 ligand and in the $S=0$ case, where the near-degeneracy of the t_{2g} states is not lifted by spin-polarization effects and different electron occupation, the degeneracy is lifted by 0.4 eV, the d_{xz} being more stable, being pushed down by the H_2O_2 LUMO (the O–O bond of the H_2O_2 ligand is lying in the xz plane). Therefore there is only one ground state electronic configuration with the d_{xz} orbital doubly occupied for $S=2$. As a consequence, similarly to the hexa-aqua complex, in the high-spin state the H_2O_2 and the H_2O ligands along the z axis have the Fe–O bonds elongated with respect to the other ligands.

By comparing Figure 3 and Figure 1, we note that the H_2O_2 has a different orientation than the H_2O it replaces. This is an interesting feature of the ground state geometry of **1**: in fact the orientation of the O–O bond in the xz plane allows for a hydrogen bond interaction between O7 and H10 (see Figure 3). The O7–H10 bond length (of 1.91 Å for $S=0$ and 2.06 Å for $S=2$) (see Table 2) is close to the hydrogen bond (1.91 Å) in the water dimer. By rotating the O–O bond by 90° around the z axis, while fixing the other geometrical parameters, we have estimated that this interaction gives a stabilization of about 3 kcal mol^{-1}, slightly less than the H-bond in $(H_2O)_2$. The comparison of the geometry of H_2O_2 in **1** and in the vacuum (see Table 2) shows that the O–O bond is a little elongated in the complex for $S=2$ and strongly elongated for $S=0$. Furthermore this result can be interpreted with the electronic structure. The uppermost molecular orbitals in the complex **1** are similar to those of the hexa-aqua complex. However, while in the hexa-aqua complex the LUMO orbitals of the water ligands do not have any overlap with the iron d states, we observe that the LUMO of the H_2O_2 ligand in **1** is much lower in energy and has a significant overlap with the d_{xz} orbital. This is evident in Figure 4 which shows the highest occupied orbital in the $S=2$ state (classified as $28a^{\downarrow}$ in Table 5): Note the $p_\sigma - p_\sigma$ antibonding character

Table 5. One-electron energies and percent composition of the lowest unoccupied and highest occupied molecular orbitals of $[Fe^{II}(H_2O)_5H_2O_2]^{2+}$ in the $S=2$ state in terms of Fe, water and hydrogen peroxide fragments.

Orbital	ε [eV]	Fe	H_2O	H_2O_2
	occupied orbitals			
27a ↑	−15.92	3 d_{xy}, 43 d_{yz}	34 HOMO waters along y	5 HOMO
28a ↑	−15.82	42 d_{xy}, 5 d_{yz}	48 HOMO waters along x	
29a ↑	−15.51	4 d_{z^2}, 3 d_{yz}		66 HOMO − 1, 20 HOMO
27a ↓	−15.46			50 HOMO − 1, 46 HOMO
30a ↑	−15.08	9 d_{z^2}, 51 $d_{x^2-y^2}$	20 HOMO − 1 waters in the (xy) plane	11 HOMO
31a ↑	−14.87	85 d_{xz}	6 HOMO waters along z	
32a ↑	−14.40	17 $d_{x^2-y^2}$, 48 d_{z^2}	10 HOMO − 1 waters along x	15 HOMO
28a ↓	−12.93	91 d_{xz}	2 HOMO waters along z	5 LUMO
	unoccupied orbitals			
29a ↓	−12.38	65 d_{xy}, 27 d_{yz}	3 HOMO waters along x	
30a ↓	−12.28	28 d_{xy}, 67 d_{yz}	3 HOMO waters along y	
31a ↓	−11.67	59 $d_{x^2-y^2}$, 26 d_{z^2}	7 HOMO − 1 waters along y	15 HOMO
32a ↓	−10.67	25 $d_{x^2-y^2}$, 44 d_{z^2}		18 LUMO
33a ↑	−10.36			89 LUMO
33a ↓	−10.22			85 LUMO
34a ↑	−9.19	22 4s	65 LUMO	LUMO, LUMO + 1
34a ↓	−9.04	4s	LUMO	LUMO, LUMO + 1

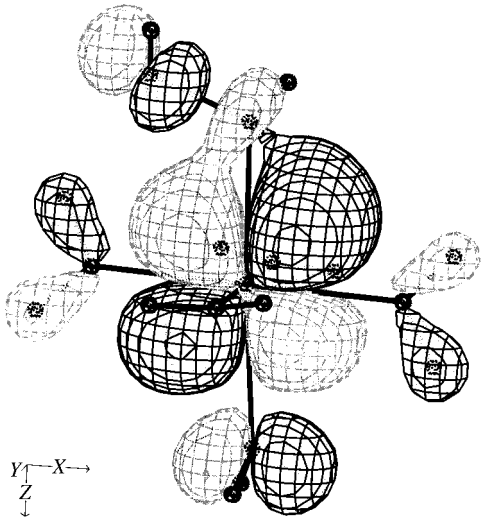

Figure 4. HOMO of the primary intermediate $[Fe^{II}(H_2O)_5H_2O_2]^{2+}$ (**1**). Notice the π-type overlap between the d_{xz} orbital and the $p_\sigma - p_\sigma$ antibonding LUMO of the hydrogen peroxide. Black and grey surfaces correspond to negative and positive lobes of the orbital, respectively.

(p_σ is oriented along the O–O bond axis) of the LUMO of H_2O_2 and the π-type overlap through the O6 – p_σ with d_{xz}. The elongation of the O–O bond would then be a consequence of the O–O antibonding nature of the LUMO of H_2O_2 (see Table 3). This is a remarkable feature which is related to the catalytic effect of the metal center in the O–O bond cleavage of hydrogen peroxide, as will be discussed in the following. In Table 5 we notice also the appearance of a molecular orbital with an energy which falls within the d manifold, which contributions are mainly from the HOMO and HOMO – 1 of the H_2O_2 ligand. This is a consequence of the fact that the HOMO and HOMO – 1 of H_2O_2 are higher in energy than those of H_2O.

The computed Mulliken charge on the Fe ion (nominal charge 2+) is +0.90 for the $[Fe^{II}(H_2O)_5H_2O_2]^{2+}$ complex, which is approximately the same as in the $[Fe^{II}(H_2O)_6]^{2+}$ complex. However, while the donating orbital of the water ligands is the σ_{lp} (0.19 electrons per water), there are two donating orbitals in the H_2O_2, namely the HOMO and the HOMO – 2 (total donation of 0.19 electrons). Moreover a small backdonation (of 0.03 electrons) occurs into the LUMO of H_2O_2.

$[Fe^{II}(H_2O)_4(OOH^-)(H_3O^+)]^{2+}$: An alternative reactive intermediate? It has been proposed that the hydroxylation of an aromatic substrate by Fenton reagents, such as the hydroxylation of benzene to phenol, does not occur through a free hydroxyl radical mechanism but rather through a reactive intermediate $[L_xFe^{II}(OOH^-)(BH^+)]^{2+}$ (**X**) obtained by nucleophilic addition of HOOH to the iron center, where L_x = bpy (bipyridine), or $OPPh_3$ (triphenylphosphine oxide) and B = py (pyridine), or H_2O.[7, 9] The formation of the active species **X** implies that after the nucleophilic addition of HOOH the first step is a proton transfer from the hydrogen peroxide to one ligand (or to the solvent) and not the O–O bond breaking. In this section we explore the possible stability of such an intermediate in the case of a ferrous complex with water ligands. The question here is whether the complex $[Fe^{II}(H_2O)_4(OOH)(H_3O)]^{2+}$ (**4**) is stable against the primary intermediate **1**. By analyzing the ground state geometry of the $[Fe^{II}(H_2O)_5H_2O_2]^{2+}$ complex (see Figure 3 and Table 2), we see that the hydrogen H18 points toward the oxygen O4 of the nearest water ligand. Therefore, it appears reasonable to generate an initial configuration for the **4** complex by displacing the proton H18 to this water ligand. The initial assumption is shown in Figure 5 (configuration I of panel a)

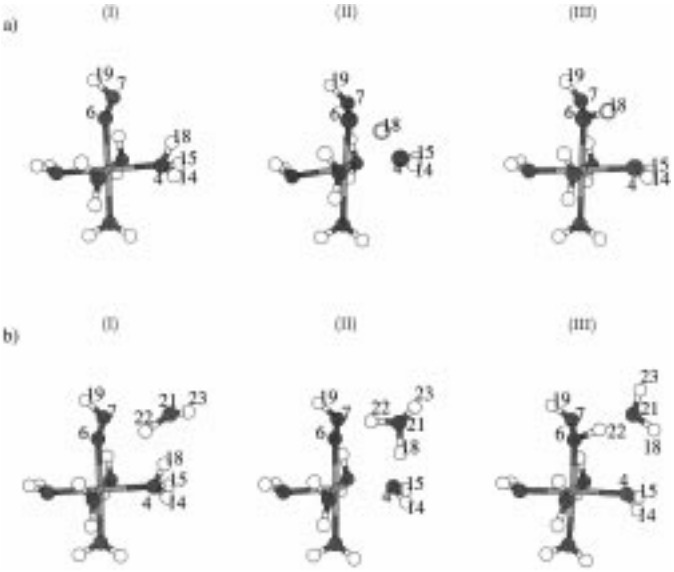

Figure 5. Geometry optimization of $[Fe^{II}(H_2O)_4OOH(H_3O)]^{2+}$ without (panel a) and with an additional water molecule (panel b). The sequence of configurations from (I) to (III) along the structural relaxation shows that the proton (H18) jumps back to the hydrogen peroxide ligand.

and has an energy about 70 kcal mol^{-1} higher than the compound **1**. By performing a geometry optimization, we find that in a few steps the proton jumps back to the OOH ligand; this shows that the complex **4** is highly unstable against the intermediate **1** (Figure 5a). In addition, we have checked whether the introduction of an extra water molecule in the vicinity of the OH_3^+ ligand, to simulate the presence of the solvent, might change the relative stability. It turns out that the proton is initially transferred to the extra water molecule (Figure 5b), configuration II) and then jumps back to the OOH to form again the hydrogen peroxide ligand of the complex **1** (Figure 5b configuration III). Notice that actually a different H (H22), which is initially located on the extra water molecule, jumps to the OOH. We have found that the complex **4** is unstable both in the low-spin ($S = 0$) and high-spin ($S = 2$) states.

We can conclude that the complex **4** is not a good candidate as a reactive intermediate in the Fenton reaction, at least in the case of Fe^{2+} with water ligands.

Reaction path from $[Fe^{II}(H_2O)_5H_2O_2]^{2+}$ (1) to $[Fe^{IV}(H_2O)_4(OH)_2]^{2+}$ (2): Starting from the primary intermediate **1** we have progressively elongated the O–O bond to compute the energy needed to break this bond in the iron complex. In Figure 6 we plot the energy change with respect

  0947-6539/01/0713-2780 $ 17.50+.50/0 *Chem. Eur. J.* **2001**, *7*, No. 13

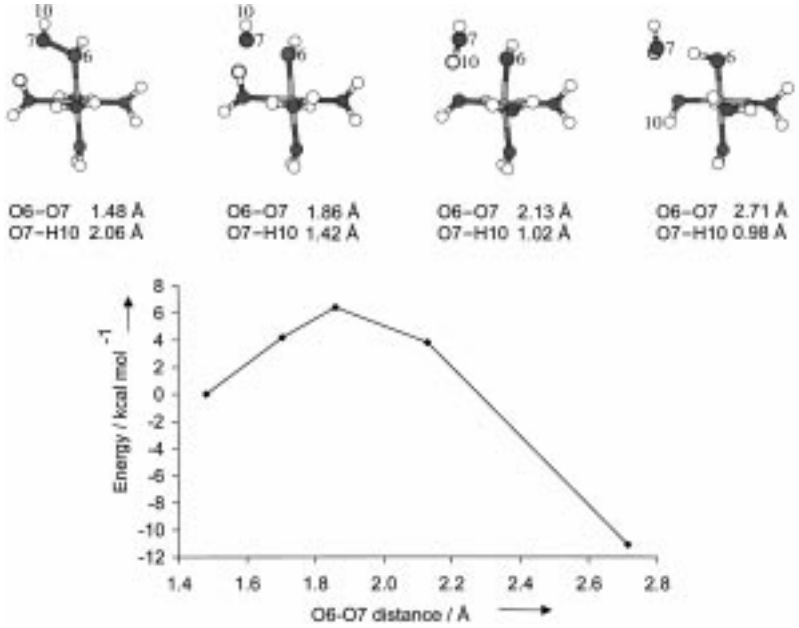

Figure 6. The computed energy in the reaction path which transforms **1** into **2** as a function of the O–O bond length. Four configurations along the reaction path are also shown to illustrate the process, see Equation (5). The zero of the energy corresponds to the ground state energy of **1**.

to the ground state energy of **1** as a function of the O–O bond length. This result has been obtained by keeping the O6–O7 bond length fixed and optimizing all the others degrees of freedom. Four configurations are shown in Figure 6 to illustrate the reaction path. It is important to realize that while we elongate the O6–O7 bond the O7–H10 distance decreases, which implies that the hydrogen-bond interaction (which was present in the ground state between the H_2O_2 and one of the water ligands), becomes stronger. Indeed we observe that the OH radical formed as a consequence of the O–O bond breaking, abstracts a hydrogen from the water ligand involved in the hydrogen bond interaction and forms a new water molecule. Therefore in this process the OH radical is "trapped" in the complex as soon as it is formed. Schematically we observe the following reaction occurring with an energy barrier of only 6 kcal mol^{-1}, as shown in Figure 6:

$$[Fe^{II}(H_2O)_5H_2O_2]^{2+}\ (\mathbf{1}) \longrightarrow [Fe^{IV}(H_2O)_4(OH)_2]^{2+}\ (\mathbf{2}) + H_2O \qquad (5)$$

The final result is the formation of a complex with four water ligands and two OH^- ligands (**2**) plus a water molecule in the second coordination shell forming a strong hydrogen bond with one OH^- ligand. The effect of the Fe^{2+} ion in catalyzing the O–O bond breaking of hydrogen peroxide is striking: indeed the barrier to break the O–O bond in the complex **1** is an order of magnitude smaller than the energy cost to break this bond in H_2O_2 in the vacuum, and the total reaction is even exothermic. These findings can be rationalized in view of the formation of Fe–OH bonds which are stronger than the Fe–H_2O bonds. In fact, the computed Fe–O bond lengths for the two OH ligands in **2** are 1.75 Å and 1.77 Å, thus much shorter than the computed Fe–O bond length for the four water ligands in the same complex, which are 2.07 Å (×2) and 2.22 Å (×2). In order to obtain a quantitative estimate of the Fe–OH bond dissociation energy, we have considered the complex $[(H_2O)_5Fe^{III}(HO)]^{2+}$ and the two fragments $[(H_2O)_5Fe]^{2+}$ and ·OH. We find a dissociation energy of 60 kcal mol^{-1}, which is 35 kcal mol^{-1} higher than the Fe–H_2O FBDE computed for the hexa-aqua-Fe^{2+} complex. Therefore, the energy gain involved in the formation of the two OH^- ligands can fully balance the energy cost of the HO–OH bond breaking.

Moreover, the comparison of the total bonding energy of **1** with the two fragments $[(H_2O)_5Fe^{III}(HO)]^{2+}$ and ·OH gives an energy of 27 kcal mol^{-1} to break the HO–OH bond and move the ·OH radical at infinite distance. This result is consistent with the cost of the O–O bond breaking (62 kcal mol^{-1} in the vacuum) and the gain in the formation of one Fe–OH metal ligand bond instead of the Fe–H_2O_2 bond. This energy of 27 kcal mol^{-1} is much higher than the energy barrier observed in Figure 6, and suggests that it is very unlikely that the OH radical can move into the solvent. Instead the abstraction of a hydrogen from one water ligand leads to the formation of a second Fe–OH bond which makes the whole reaction exothermic. Indeed, we have also checked that even if two extra water molecules are added in the vicinity of the complex **1**, the reaction path illustrated in Figure 6 is unchanged and the hydroxyl radical is immediately trapped in the iron complex.

The existence of a highly reactive iron intermediate $[Fe(OH)_2]^{2+}$ has been actually proposed in the literature as being formed in the reaction between hydrogen peroxide and a Fe^{II} complex with HEDTA (hydroxyethylethylenediaminetriacetic acid) ligands.[6]

We find that the ground state of the complex **2** is a d^4 high spin configuration $S = 2$ with a d electron distribution which can be schematically described as $d_{xy}^{\uparrow}\, d_{xz}^{\uparrow}\, d_{yz}^{\uparrow}\, d_{x^2-y^2}^{\uparrow}$, (when the OHs are along the x and z axis) though partial occupation of the other d orbitals occurs. During the reaction **1** → **2** the nominal oxidation state of iron goes from Fe^{II} to Fe^{IV}. However the actual Mulliken charge on the Fe ion (Z minus electrons) goes from $Q(Fe)_{\mathbf{1}} = 0.90$ to $Q(Fe)_{\mathbf{2}} = 1.16$. Although nominally the electrons are transferred from the $d_{xz}^{\downarrow}$ and $d_z^{2\uparrow}$ orbitals to the two OH ligands to produce the formally OH^- ligands, there is so much rearrangement in the composition of the remaining occupied $^3d^2$ orbitals that effectively the total d electron population changes very little: the total d electron population goes from 6.42 in **1** to 6.22 in **2**.

Transition state analysis: The transition state (TS) is found at a O6–O7 distance of 1.86 Å with an energy barrier of about 6 kcal mol^{-1} (see Figure 6). This small energy barrier can be also rationalized in view of the nature of the HOMO of the **1**

  0947-6539/01/0713-2781 $ 17.50+.50/0

complex which, as discussed above, has a component of the antibonding LUMO of H_2O_2. In fact the elongation of the O–O bond induces a stabilization of the LUMO of H_2O_2. At the TS, the HOMO of the complex acquires a stronger component from the LUMO of H_2O_2 and loses most of the d_{xz} character which it had in the ground state. This signifies increasing down-spin population in the π_x orbital of O_6, which ultimately will become (at least formally) doubly occupied with one up-spin electron that remains after the O–O bond breaking, and one down-spin electron that is transferred from the down-spin d_{xz} orbital by changing the character of the relevant orbital from (mostly) d_{xz} to (mostly) H_2O_2 π_x. The Fe–O6 and Fe–O2 bonds gets stronger with bond lengths of 1.92 Å and 2.00 Å, respectively, while the other Fe–O distances are ≈2.15 Å. The O7–H10 bond length decreases to 1.42 Å and correspondingly the O2–H10 bond elongates to 1.08 Å. At the TS the dynamical matrix exhibits a single imaginary mode (negative frequency) which is characterized by the stretching of the O6–O7 bond and the concomitant shortening of the O7–H10 bond length. The Mulliken charge analysis shows that the O7H19 fragment is indeed a radical with a spin density of −0.43, in agreement with the bond breaking ultimately leading to a down-spin electron on the leaving OH and an up-spin electron left behind on the coordinated OH. In the transition state we indeed find the negative spin density on the leaving OH radical to be compensated by a spin density increase on the complex distributed over the iron and the oxygen atoms. The charge on iron is $Q(\mathrm{Fe})_{TS} = 1.02$.

Reaction path from $[Fe^{IV}(H_2O)_4(OH)_2]^{2+}$ (2) to $[Fe^{IV}(H_2O)_5O]^{2+}$ (3): As already mentioned, an alternative mechanism in the Fenton reaction proposed by Bray and Gorin[15] involves an oxo complex $Fe^{IV}O^{2+}$ as the key intermediate. This complex can be formed from the primary intermediate **1** by the loss of a water.[11] The stoichiometry of the reaction is:

$$[Fe^{II}(H_2O)_5H_2O_2]^{2+}\ (\mathbf{1}) \longrightarrow [Fe^{IV}(H_2O)_5O]^{2+}\ (\mathbf{3}) + H_2O \qquad (6)$$

In the previous section we have described a reaction path from **1** to **2** which results in the loss of a water molecule and the formation of two OH ligands. A process is conceivable which transforms complex $[Fe^{IV}(H_2O)_4(OH)_2]^{2+}$ (**2**) into complex $[Fe^{IV}(H_2O)_5O]^{2+}$ (**3**) by transferring a proton from one OH ligand to the other. Indeed we find that **3** is preferred (in the vacuum) by about 9 kcal mol^{-1} over the complex **2**. Once again in the complex **3** the high spin $S = 2$ state is the lowest in energy. In order to compute the energy barrier involved in the proton transfer which transforms **2** into **3**, we have performed geometry optimizations at fixed OH distances, progressively displacing one proton from one OH ligand to the other: Along this reaction path we obtain an energy barrier of about 22 kcal mol^{-1}. This barrier seems too high for a spontaneous occurrence of this reaction.

However, this process can occur more easily in the presence of an additional water molecule in the second coordination shell of **2**, as illustrated in Figure 7. A strong interaction arises between the extra water molecule and one of the OH ligands. After geometry optimization the proton (H18) of the OH ligand moves in a bridging position between O6 and O7 (first configuration shown in Figure 7). The total energy of this configuration is about 24 kcal mol^{-1} lower than the intermediate **1**. We then progressively reduce the distance between

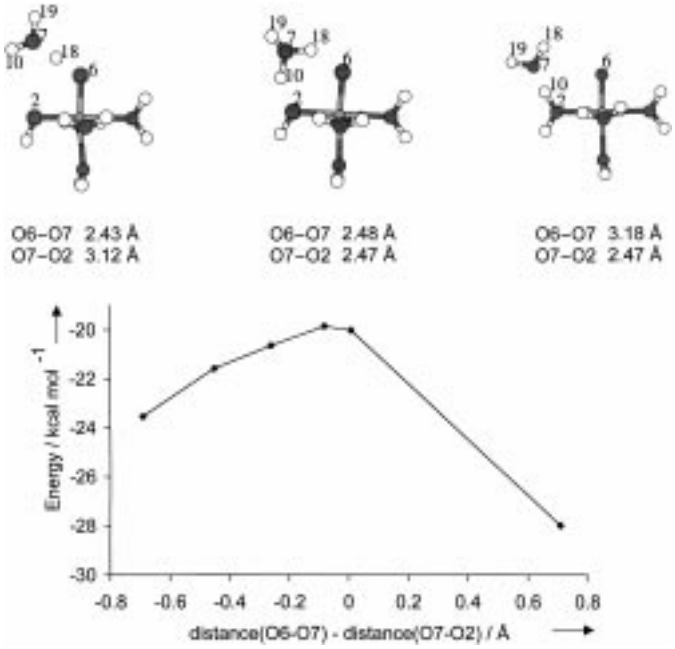

Figure 7. The computed energy in the reaction path which transforms **2** into **3** with the inclusion of an additional non-coordinated water molecule, see Equation (3). Three configurations are shown to illustrate the reaction. The zero of the energy is the same as in Figure 6.

O7 and O2 while relaxing all the other degrees of freedom. We plot the energy as a function of the difference between the O6–O7 and O7–O2 bond lengths. First the proton (H18) is transferred to the extra water with the formation of an OH_3^+ ion (the Mulliken charge on the OH_3^+ complex is +0.73). Then the OH_3^+ ion rotates so that a proton (not the same H18 but a different proton) can jump to the other OH ligand and form again a water ligand. The whole proton transfer process along this reaction path involves only small atomic displacements and occurs with an activation energy of only 3.5 kcal mol^{-1}. The energy barrier is thus dramatically reduced by the presence of the extra water molecule. Therefore we conclude that in the presence of the aqueous solvent the secondary intermediate **2** can easily further decay to the most stable $[Fe^{IV}(H_2O)_5O]^{2+}$ complex. The total energy gain in the two-step process from **1** to **3** is 28 kcal mol^{-1}.

The d orbitals population is similar to that of the complex **2**, though in **3** the d_z^2 orbital is pushed to higher energy. The average Fe–O_{water} bond length in **3** is 2.11 Å, while the Fe=O distance is 1.63 Å, which is shorter than in the Fe–OH bond. We estimated a bonding dissociation energy of 117 kcal mol^{-1} in going from $[(H_2O)_5FeO]^{2+}$ to $[(H_2O)_5Fe]^{2+}$+O, which is about twice the Fe–OH bond energy. Finally we note that while in the primary intermediate **1** the net spin density is localized on the iron, in **3** about 20% of the total spin density is localized on the oxygen ligand.

0947-6539/01/0713-2782 $ 17.50+.50/0 *Chem. Eur. J.* **2001**, *7*, No. 13

Conclusion

By means of density functional theory we have investigated the nature of the oxidative agent in the Fenton reaction. Starting from a primary intermediate $[Fe^{II}(H_2O)_5H_2O_2]^{2+}$ (**1**), we have shown how the Fe^{II} ion in water can catalyze the O–O bond cleavage of hydrogen peroxide. Indeed the O–O bond breaking process becomes exothermic overall and the TS barrier for breaking the O–O bond is only 6 kcal mol^{-1} in the iron complex, which is an order of magnitude lower than the energy required in the gas phase to break the bond. This is in line with the orbitally allowed character of the transformation. The net exothermicity of the O–O bond breaking can be interpreted on the basis of the replacement of two Fe–OH_2 bonds in **1** with two stronger Fe–OH bonds in **2**. The hydroxyl radical, obtained by the oxygen–oxygen bond breaking, can abstract a hydrogen atom from one of the water ligands forming a new water molecule. With this mechanism the ferrous complex **1** decays to a high valence iron intermediate **2** with two OH ligands ($\rightarrow [Fe^{IV}(H_2O)_4(OH)_2]^{2+}$), plus the loss of a water molecule. The total bond breaking process and formation of the complex **2** is actually exothermic by 23 kcal mol^{-1} (see Figure 7).

The intermediate **2** can further decay to a more stable ferryl oxo-complex $[Fe^{IV}(H_2O)_5O]^{2+}$ (**3**), by transferring a proton from one of the OH ligands to the other. This reaction path has a very small activation energy when an extra water molecule is present in the second coordination shell, and demonstrates the relevance of the solvent in this process. The total energy gain in going from **1** to **3** is 28 kcal mol^{-1}.

The results presented here show that an high valent ferryl complex $Fe^{IV}O^{2+}$ is easily formed in water and this may be the active intermediate in the oxidation reaction as first proposed in ref. [15] Of course we should be aware that the efficiency and the selectivity in the product formation in the Fenton chemistry are a function of the metal complex, the hydrocarbon substrate, and of the solvent matrix. Therefore it is possible that different active species are produced in different experimental setups. Specifically, we have found that the water environment is crucially involved in the formation of the ferryl complex. Thus, the presence of different ligands and/or solvent might modify this picture. This is an important point which needs further theoretical investigations. The reactive oxidant may be the free hydroxyl radical under certain conditions (ligands, pH, metal) and a metal-oxo complex under other conditions. However, at this stage the alternative scenario in which the OH radical obtained from the hydrogen peroxide dissociation reacts with a water molecule in the solvent—instead of the water ligand—and then diffuses toward the substrate, seems energetically unlikely. We have already preliminarily explored this scenario by including two extra water molecules close to the Fe complex and we obtained the same complex **2** as before. However, finite temperature simulations with an explicit inclusion of the solvent are indeed needed to evaluate the effect of the solvent for the reaction mechanism proposed here and to reach a more robust answer on the alternative scenario mentioned above. These calculations will be presented elsewhere.

Acknowledgements

Support from the Netherlands' Priority Programme for Materials Research (Computational Materials Science section) is gratefully acknowledged. Computing budgets for the calculations performed at the Stichting Academisch Rekencentrum Amsterdam (SARA) have been made available by the foundation Nationale Computerfaciliteiten (NCF) of the Netherlands' Foundation for Scientific Research (NWO) and by the Vrije Universiteit. We are very grateful to M. Bickelhaupt for the many helpful discussions.

[1] H. J. H. Fenton, *J. Chem. Soc.* **1894**, *65*, 899–910.
[2] For a review, see for example: P. Wardman, L. P. Candeias, *Radiat. Res.* **1996**, *145*, 523–531.
[3] a) C. Walling, *Acc. Chem. Res.* **1998**, *31*, 155–157; b) D. T. Sawyer, *Coord. Chem. Rev.* **1997**, *165*, 297–313; c) D. T. Sawyer, A. Sobkowiak, T. Matsushita, *Acc. Chem. Res.* **1996**, *29*, 409–416.
[4] F. Haber, J. Weiss, *Proc. R. Soc. London* **1934**, *A147*, 332–351.
[5] W. G. Barb, J. H. Baxendale, P. George, K. R. Hargrave, *Trans. Faraday Soc.* **1951**, *47*, 462–500.
[6] J. D. Rush, W. H. Koppenol, *J. Inorg. Biochem.* **1987**, *29*, 199–215.
[7] D. T. Sawyer, C. Kang, A. Llobet, C. Redman, *J. Am. Chem. Soc.* **1993**, *115*, 5817–5818.
[8] D. A. Wink, R. W. Nims, J. E. Saavedra, W. E. Utermahlen Jr., P. C. Ford, *Proc. Natl. Acad. Sci. USA* **1994**, *91*, 6604–6608.
[9] J. P. Hage, A. Llobet, D. T. Sawyer, *Bioorg. Med. Chem.* **1995**, *3*, 1383–1388.
[10] a) C. Kim, K. Chen, J. Kim, L. Que Jr., *J. Am. Chem. Soc.* **1997**, *119*, 5964–5965; b) R. Y. N. Ho, G. Roelfes, B. L. Feringa, L. Que, *J. Am. Chem. Soc.* **1999**, *121*, 264–265.
[11] M. L. Kremer, *Phys. Chem. Chem. Phys.* **1999**, *1*, 3595–3605.
[12] M. J. Burkitt, *Free Radical Res. Commun.* **1993**, *18*, 43–57.
[13] R. P. Mason, P. M. Hanna, M. J. Burkitt, M. B. Kadiiska, *Environ. Health Perspect.* **1994**, *102*, 33–36.
[14] J. Halperin, H. Taube, *J. Am. Chem. Soc.* **1952**, *74*, 380.
[15] W. C. Bray, M. H. Gorin, *J. Am. Chem. Soc.* **1932**, *54*, 2124–2125.
[16] See for example, the reviews in: *Metal-Oxo and Metal-Peroxo Species in Catalytic Oxidations* (Ed.: B. Meunier), Structure and Bonding, *Vol. 97*, Springer Verlag, Berlin, **2000**.
[17] See for example: R. M. Dreizler, E. K. U. Gross, *Density Functional Theory. An approach to the Quantum Many-Body Problem*, Springer Verlag, Berlin, **1990**.
[18] a) E. J. Baerends, D. E. Ellis, P. Ros, *Chem. Phys.* **1973**, *2*, 41; b) P. M. Boerrigter, G. te Velde, E. J. Baerends, *Int. J. Quantum. Chem.* **1988**, *33*, 87; c) C. Fonseca Guerra, J. G. Snijders, G. te Velde, E. J. Baerends, *Theor. Chem. Acc.* **1998**, *99*, 391.
[19] J. P. Perdew, J. A. Chevary, S. H. Vosko, K. A. Jackson, M. R. Pederson, D. J. Singh, C. Fiolhais, *Phys. Rev. B* **1992**, *46*, 6671–6687.
[20] A. D. Becke, *Phys. Rev. A* **1988**, *38*, 3098.
[21] J. P. Perdew, *Phys. Rev. B* **1986**, *33*, 8822.
[22] B. S. Brunschwig, C. Creutz, D. H. Macartney, T.-K. Sham, N. Sutin, *Faraday Discuss. Chem. Soc.* **1982**, *74*, 113–127.
[23] Actually small displacements of the hydrogen atoms out of the symmetry planes break this symmetry. However, the energy gain involved in this distorsion is very small.
[24] P. E. M. Siegbahn, R. H. Crabtree, *J. Am. Chem. Soc.* **1997**, *119*, 3103–3113. In this paper the authors using a B3LYP functional find the six-coordinate complex preferred by 8 kcal mol^{-1} over the five-coordinate.
[25] B. M. Gimarc, *J. Am. Chem. Soc.* **1970**, *92*, 266–275.
[26] See, for example: Table 7.1 in T. W. G. Solomons, *Organic Chemistry*, Wiley, New York, **1992**.
[27] W. C. Oelfke, W. Gordy, *J. Chem. Phys.* **1969**, *51*, 5336–5343.

Received: November 22, 2000 [F2888]